Journal of Materials Chemistry

Cite this: J. Mater. Chem., 2011, 21, 6707

www.rsc.org/materials

View Online
Dynamic Article Links

PAPER

Mechanics of coordinative crosslinks in graphene nanocomposites: a first-principles study

Yilun Liu, Bo Xie and Zhiping Xu*

Received 20th January 2011, Accepted 3rd March 2011
DOI: 10.1039/c1jm10300h

Published on 30 March 2011 on http://pubs.rsc.org | doi:10.1039/C1JM10300H
Downloaded by Tsinghua University on 28 April 2011

Graphene-based nanocomposites have recently received rising interest owing to their outstanding performance. Crosslinkers, such as a divalent ion based coordinative complex, have been proved to significantly improve load transfer between adjacent graphene sheets, which subsequently defines the overall mechanical properties of the composites. In this paper, the structures and mechanical properties of both interlayer and intralayer coordinative bonds are quantified through density functional theory based first-principles calculations. The structural deformation and failure mechanism are investigated under interlayer sliding and separation loads. Extensive discussion is made by comparing coordinative bonds with other types of crosslinks such as covalent bonds, van der Waals interactions and hydrogen bonds. Moreover, the impacts from the crosslink mechanisms to overall properties of nanocomposites are projected towards the applications in high-performance multifunctional materials.

1. Introduction

High-performance and low-cost composites are engineer's dream materials for mechanical, civil and aerospace applications. The carbon fibers, as first created in the 1950's, are still major suppliers of high performance composites for their remarkable mechanical properties, relatively easy, cheap fabrication and low weight. Recently, with the development of nanoscale synthesis and engineering technologies, in addition to inspiration from hierarchical structures in biological materials, nanocomposites featuring superior stiffness, strength and energy dissipation capacities are reported as the next-generation super-materials.[1–3] For example, super-strong nanofibers, such as carbon nanotubes, are dispersed in polymer or metal matrices for mechanical reinforcement.[4] The carbon nanotubes, with perfectly cylindrical graphitic structures, attract enormous efforts towards realizing their applications in high-performance nanocomposites. However, issues such as the limited surface-to-volume ratio due to the inaccessibility of the inner wall, poor dispersion ability in the matrices due to bundle formation and also their relatively higher cost, prohibit wide applications as reinforcement phases. In contrast, graphene-based nanocomposites, or papers, impressively overcome these issues by providing two-dimensional building blocks assembled in a layer-by-layer hierarchy,[1,5] which can be further crosslinked by various chemicals to establish both interlayer and intralayer (*i.e.* graphene sheets are bridged on the edges, in the same plane) load transfer.

Computational Energetics Laboratory, Department of Engineering Mechanics, School of Aerospace, and Center for Nano and Micro Mechanics, Tsinghua University, Beijing, 100084, China. E-mail: xuzp@tsinghua.edu.cn

In graphene and its derivative based nanocomposites, graphene nano-flakes are assembled in a layer-by-layer manner. When tensile load is applied, as the stress can hardly be continuously sustained through in-plane bonds between distributed nano- or micro-flakes, the interlayer shear stress thus can be produced through crosslinks to take the responsibility for interlayer load transfer. The interlayer shear strength in a graphite crystal through van der Waals interaction is extremely low, on the order of mega-pascals, which limits the overall stiffness, strength and toughness of the whole material.[6,7] From this point of view, with modified basal-plane chemistry, such as by the epoxy and hydroxyl groups, the graphene oxide that features weakened in-plane mechanical properties but much improved interlayer interactions, shows great potential in the fabrication of high-performance nanocomposites. Recent experiments show that remarkable improvements of the mechanical properties (Young's modulus, strength and toughness) are observed through introducing various functional groups, such as divalent ions and polymers such as alkylamines.[8–12] Although these experiments validate that these approaches can systematically tune the mechanical properties of graphene-based nanocomposites through chemical treatment, the structure–mechanical property relationship at the atomic scale is still not understood, especially for the coordinative bonds assisted by intercalated divalent ions such as Mg^{2+} and Ca^{2+}, as reported in ref. 10. Optimal designs by engineering the hierarchical structures of graphene-related materials are thus prohibited by missing the key mechanical parameters such as the tensile (shear) modulus and strength.

Coordinative bonds, which are created by the provision of an electron pair by one of the binding partners (the ligand) for a binding interaction, are usually found with metal atoms and

View Online

Published on 30 March 2011 on http://pubs.rsc.org | doi:10.1039/C1JM10300H
Downloaded by Tsinghua University on 28 April 2011

ions exhibiting unoccupied orbitals.[13] The coordinative complex usually features both ionic and dipole–dipole interactions. These bonds have been widely utilized by biological materials to enhance their mechanical properties. Evidence is found in the stabilization of heme pigment in blood cells, and also that metal ion coordination can be engineered to regulate amyloid fibril assembly and toxicity.[14] In general, the strength of a coordinative complex covers a wide range, lying between weaker dipole–dipole interactions as encountered in van der Waals interactions and hydrogen bonds, and stronger covalent bonds, according to the complexities of coordinative interactions and compounds thus formed. Despite these unique features of coordinative bonds and reported structural information, their mechanical properties and roles in improving load transfer processes in nanocomposites are not clarified yet.

2. Methods

2.1 First-principles calculations

Although empirical potential functions or forcefields with parameters are widely used in the atomistic simulation to describe the interatomic interaction of a wide range of organic and inorganic materials, a quantitative prediction of coordinative bonds has not been implemented in this way; especially at non-equilibrium condition where atomic structures are distorted from their equilibrating ones to material failure, the electron transfer or redistribution must be taken into account. In this work, we establish it through utilizing quantum mechanics based first-principles calculations in evaluating energy and force of atomic structures.

The interface between a bilayer graphene sheet with various functional groups is investigated through a rhombic supercell of 1.72 nm × 1.72 nm. The cell size chosen here is used to ensure the exclusion of the interaction between one coordinative group and its periodic image in the neighboring cell, which determines the maximal crosslink density in this method. As the distortion of the graphene lattice due to a crosslink is localized, mechanical properties of larger supercells with reduced crosslink densities can thus be simply deduced by area conversion. A vacuum layer of 2 nm is used in the direction normal to the interface, representing the isolated boundary condition for the graphene bilayer. The structure and property of this hybrid system are subsequently investigated using plane-wave basis set based Density Functional Theory (DFT) methods. Generalized Gradient Approximation (GGA) in PBE parameter settings is used for the exchange–correlation functional and Projector Augmented Wave (PAW) potentials are used for ion–electron interaction. We use the Vienna Ab-inito Simulation Package (VASP) for the calculations. For all results presented, an energy cut-off of 300 eV is used for the plane-wave basis sets. A gamma point is used for the Brillouin zone integration as we have a large supercell. These settings have been verified to achieve a total energy convergence less than 1 meV atom^{-1}. For geometry relaxation, the force on atoms is converged below 0.01 eV Å^{-1}. All structures are initially optimized using a conjugated gradient method. It should be noted that in our simulation a supercell is used. Thus here the model actually represents graphene papers with a periodic crosslink array, the density is one crosslinker per 2.562 nm^2. The equilibrium structure is thus determined by a combined optimization of both local structural adjustment of the coordinative complex and the induced distortion in graphene sheets, which is dependent on the supercell size. The size of supercell chosen here is ensured to exclude this dependence.

2.2 Mechanical properties characterization

Tensile behaviors of graphene sheets or graphene sheets connected by intralayer crosslinkers are investigated by directly applying in-plane tensile deformation on the supercell (for bilayer graphene sheet) in one direction and geometrical optimization afterwards for both atomic positions and supercell dimensions in the other two directions. The stress is calculated by assuming the graphene sheet is a thin shell with a thickness of 1 nm. The performance of interlayer crosslinkers is measured by vertically (transversely, in both <1$\bar{1}$00> and <11$\bar{2}$0> directions) moving one layer of graphene sheet with respect to its neighbor step by step. After shear displacement is applied, the degrees of freedom of all carbon atoms in the shear direction are fixed, while the other two directions are set to be freely relaxed for subsequent geometrical optimization calculations. The interlayer stress is calculated by summing up all forces acting on the carbon atoms of one graphene layer in the shear direction, and then being divided by the area of the supercell in use. Similarly, the cohesive stress, or tensile stress along the normal direction <0001>, is calculated by summing up all forces in that direction.

3. Results

3.1 Atomic structures

Interlayer crosslink. The optimized structures of graphene sheets with coordinative bond bridges on the surface or edges are depicted in Fig. 1(a) and (b) in atomic representations. The interlayer crosslink type, (a), is the alkoxide, or dative, coordination as predicted from experiments,[10] denoted as structure I. The divalent ion (magnesium here) is bound to negatively charged oxygen atoms as ligands, providing electron pairs, which belong to epoxy or hydroxyl groups on the graphene sheets. As its electron configuration is [Ne]3s^2, a maximum of three pairs can be accepted. The magnesium atom bridges two oxygen atoms in the epoxy groups, and one oxygen atom in a hydroxyl group, both bound to the graphene sheets. The hydroxyl and epoxy group are aligned in the <1$\bar{1}$00> (or armchair) direction of the graphene lattice and the three oxygen atoms nearly form a plane including the magnesium atom. For structure I, the Mg–O bond lengths are 0.187 (oxygen atom in a hydroxyl group), 0.189 and 0.193 nm (oxygen atoms in epoxy groups), respectively. For reference, the summation of the covalent radius of magnesium and oxygen is 0.207 nm. The interlayer distance here has been expanded from 0.336 nm for graphite to 0.709 nm, close to the measured value of 0.86 nm in the rinsed Mg-modified graphene oxide paper.[10,15] In comparison to single layer graphene oxide, the structures of epoxy and hydroxyl groups here are distorted due to the coordination with magnesium. Due to the binding between the oxygen atoms in the epoxy groups and the magnesium, one C–O bond in the epoxy groups is broken, leaving a single C–O bond of 0.144 nm, instead of 0.147 nm in the epoxy group. The hydroxyl group that is initially bound to the graphene

 This journal is © The Royal Society of Chemistry 2011

View Online

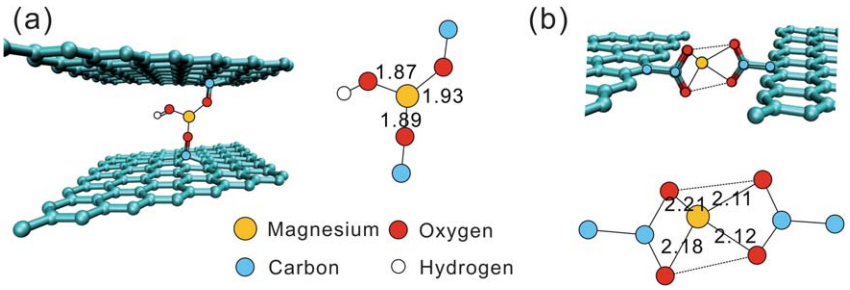

Fig. 1 Structures of divalent ion based crosslinks that bridge graphene sheets. (a) Is an interlayer crosslinker as reported in ref. 10. The bond lengths in the local structures are depicted in Å. (b) Is the intralayer crosslink that provides a coordinative connection between oxygen atoms in neighboring graphene sheets and the magnesium atom buckles out of the plane. These two structures show Mg–O bond lengths between 0.19 to 0.21 nm.

Published on 30 March 2011 on http://pubs.rsc.org | doi:10.1039/C1JM10300H
Downloaded by Tsinghua University on 28 April 2011

sheet is detached by the strong coordinative interaction in the Mg–O complex, with an O–H distance of 0.097 nm.

Since the positions of the epoxy and hydroxyl groups at the attaching points will apply additional constraints on the geometry optimization of the coordinative complex, the structure optimized here is the local minimum of the energy profile, not always the global minimum. More discussion on this issue can be found in following sections where whole energy profiles under external loads are revealed.

Intralayer crosslink. In addition to the interlayer crosslinkers connecting basal planes of graphene sheets, alkaline earth metals can also strongly bind the graphene sheets at their edges, as a carboxylic acid group. Two oxygen atoms are bridging the metal atoms from two sides, to the carbon atoms connected to the zigzag edges of the graphene sheets.[10] In our calculation, the magnesium atom is found to move out of the plane formed by four oxygen atoms belonging to the Mg–O complex after geometry optimization, and the carbon–oxygen bonds have lengths ranging from 0.21 to 0.22 nm.

3.2 Resistance to interlayer sliding, shear modulus and strength

When shear load is applied on structure I, the coordinative complex deforms before structural failure where the Mg–O bond breaks. As depicted in Fig. 2(a) and (b), during the sliding of the top graphene layer with respect to the bottom layer in the <1$\bar{1}$00> direction, the energy profile has a harmonic shape around the global minimum (Fig. 2(a)). In the positive direction (Fig. 2(b)), the stress–strain curve keeps linearity with a shear modulus G of 0.97 GPa when the displacement is below 0.28 nm, beyond which the behavior is stiffened ($G = 2.11$ GPa) before the breakage of the Mg–O bond at $\tau_s = 799$ MPa, as the O–Mg–O chain is straightened. However, as the sliding is in the negative direction (towards the hydroxyl group), the energy profile drops firstly by 0.1 eV at −0.28 nm displacement, representing a structural transition as illustrated in Fig. 2(c) and labeled as "C". The oxygen atom needs to move over the magnesium atom. When further loaded after the transition, the structure also fails at the point where the Mg–O bond breaks, with a slightly higher shear modulus of 2.32 GPa and strength τ_s of 811 MPa. The energy barrier for the breaking of the Mg–O bonds here is 1.5 and 1.6 eV, respectively. The structural deformation of the coordinative complex under shear load here suggests that the mechanical

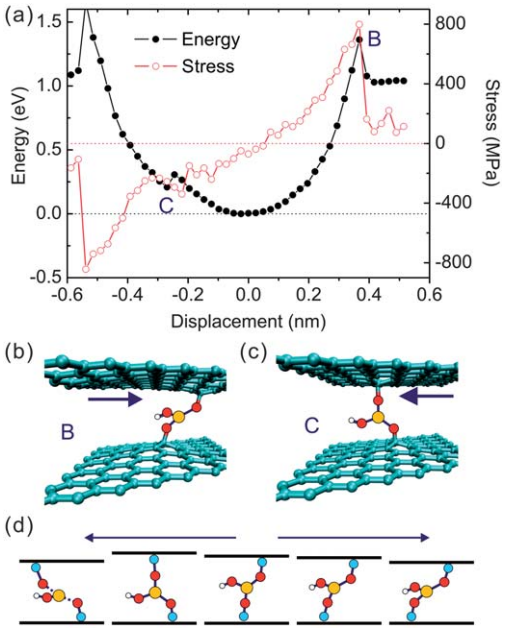

Fig. 2 Resistance to interlayer sliding of structure I. (a) Energy and stress profiles as the top graphene layer is moved in both positive (B) and negative (C) directions. In the positive direction (b), the structure fails as the Mg–O bond breaks. In the negative direction, firstly the oxygen atom bound to the top layer needs to jump over the magnesium atom underneath (c), which corresponds to an energy drop. The shear displacements in (b) and (c) are labeled in (a) with B and C. (d) A sequence of snapshots showing the structural changes from displacement at −0.54, −0.27, 0.0, 0.27, to 0.37 nm.

performance is mainly carried by the magnesium–oxygen bond. Based on this assumption, the strength of the Mg–O bond is quantified to be 2 nN along the <1$\bar{1}$00> direction. The maximum shear strains before bond breaking correspondingly are 0.52 and −0.76 in the two <1$\bar{1}$00> directions. The same calculations are also performed for shear loads in the <11$\bar{2}$0> direction, the shear strength and energy barrier are 516 MPa and 1.4 eV, respectively.

3.3 Resistance to interlayer separation and binding strength

The binding energy and stress for the coordinative complex mediated graphene bilayer is also investigated in the direction normal to the basal plane by separating adjacent graphene

View Online

Published on 30 March 2011 on http://pubs.rsc.org | doi:10.1039/C1JM10300H
Downloaded by Tsinghua University on 28 April 2011

sheets. For structure I the energy calculated is 1.4 eV and the cohesive strength is 1.011 GPa. As no structural transition is observed in the tensile process, a smooth stress–strain curve is obtained (Fig. 3), that is linear initially with an elastic modulus of 6.22 GPa in the tensile direction and slightly softening before Mg–O bond breaking at strain 0.18. The Mg–O bond strength calculated here is 2.53 nN.

3.4 Enhancement of intralayer mechanical properties

For the intralayer crosslinked structure II, a magnesium atom is sandwiched between four oxygen atoms. At a displacement of 0.05 nm, the magnesium atom that initially buckles out starts to be pulled back from the out-of-plane position to the plane formed by the four oxygen atoms (Fig. 4(b)). Correspondingly, the stress–displacement curve features a flat region before stiffening again as the magnesium atom is in the plane (labeled as "B" in Fig. 4(a)). When the displacement further exceeds 0.2 nm, one Mg–O (labeled as "1" in Fig. 4(c)) breaks at first. The structure eventually fails at 0.25 nm, where the other Mg–O bond breaks in sequence (labeled as "2" in Fig. 4(c)). As interpolated from the tensile stress–strain curve, the tensile modulus and strength of the supercell are 57.4 and 2.85 GPa, by considering the thickness of the graphene sheet to be 1 nm.

4. Discussion

4.1 Comparison with other bridging mechanisms

The metal atom mediated coordinative bridging is a typical interaction involved not only in graphene based nanocomposites, but also in general macro-molecular assembly processes and nano-structural engineering, in addition to other mechanisms including covalent bonds, hydrogen bonds, van der Waals forces *etc.* To compare the coordinative interaction with others, we summarize their characteristics (energy, bond length, strength and directionality) schematically in Fig. 5. The covalent bond, forming between atoms that share electrons from both of them, is very stable, directional and can be introduced by electron irradiation.[16] The binding energy and typical bond length in bio- or macro-molecules are 2–8 eV and 0.1–0.18 nm, respectively, and the strength of a single carbon–carbon bond is around 7.3 nN.[17] The coordinative bonds, sometimes also called coordinative covalent bonds, have similar, but lower binding energy because the metal

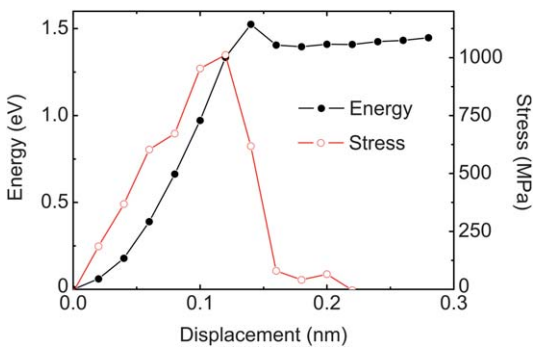

Fig. 3 Energy and tensile stress profile of coordinative bonds bridging graphene bilayers (structure I) under tensile load in the normal direction to graphene sheets.

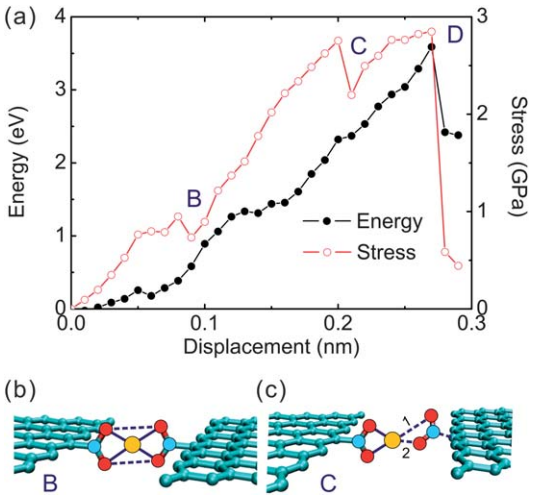

Fig. 4 (a) Intralayer energy and stress profiles of carboxylate group inter-linked graphene sheets under tensile loading. When stretched, the Mg–O complex is firstly straightened and the magnesium atom is pulled back to the plane formed by the oxygen atoms (a) at "B". The structure fails and the Mg–O bonds break in sequence (first bond "1" in (c) at "C", then bond "2" at "D"). The tension displacements in (b) and (c) are labeled in (a) with B and C.

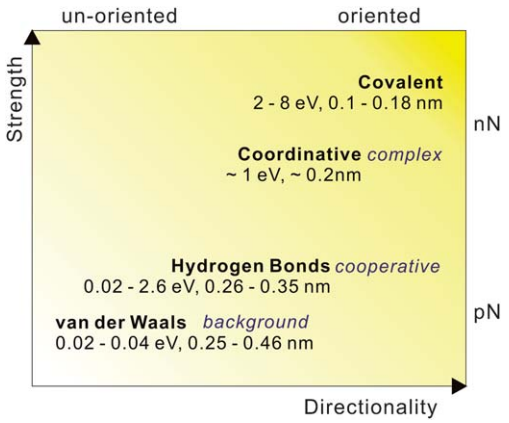

Fig. 5 Comparison of different crosslink mechanisms in graphene nanocomposites, in terms of strength and directionality. The typical energy value and bond length are also given in the units of eV and nm. The binding energy of hydrogen bonds covers both weak and strong hydrogen bonds as classified in ref. 21, the bond length is the distance between the electron donor and acceptor.

atoms usually have large sizes. In addition, the binding electron pairs come from one atom rather than both in the covalent bond. The coordinative bond is also unique in that it always forms a complex rather than a single bond. The binding energy and strength of the coordinative bonds obtained from our calculations here are ~1 eV and 2 nN. This value of Mg–O bond strength, is higher than the measured value 500 pN for the bonding strength between a Histidine tag and a Ni-Nitrilotriacetate and 750 pN with Fe(III), as quantified through single-molecule scanning force microscopy measurements.[18] By considering the periodic supercell setup and zero-temperature calculation in our work, the value should be higher than the experimental measurements where the single bond is under investigation, and thermal fluctuation could

 This journal is © The Royal Society of Chemistry 2011

View Online

Published on 30 March 2011 on http://pubs.rsc.org | doi:10.1039/C1JM10300H
Downloaded by Tsinghua University on 28 April 2011

Table 1 Typical mechanical parameters of coordinative bond crosslinked graphene bilayers

Crosslinks types		Strength (MPa)	Modulus (GPa)	Failure strain	Crosslink bond	
					Strength (nN)	Binding energy (eV)
Interlayer crosslink	Shear	811	2.32	0.76	2	1.5
	Separation	1011	6.22	0.18	2.53	1.4
Intralayer crosslink		2850	57.4	0.065	4.9	3.6

effectively lower the energy barrier for bond breaking. Also, the higher value for Mg–O coordinative bond as calculated here could arise from the smaller size of the magnesium atom to that of nickel and iron.

In addition to these two relatively strong interactions, weak bonds such as hydrogen bonds and van der Waals forces also play remarkable roles in macromolecular aggregations and nanocomposites. The hydrogen bond, representing both electrostatic and van der Waals forces between electron donors and acceptors, is a weak bond in energy (0.02–2.6 eV) and strength. However, when working cooperatively, an organized hydrogen bond network can provide outstandingly high strength,[19,20] as utilized by biological materials such as spider silks with parallel hydrogen bonds in the beta-sheet secondary structure. Unlike the hydrogen bond that is localized and oriented, the van der Waals interaction provides a background force, *i.e.* without directionality. The van der Waals force usually has a binding energy of 0.02–0.04 eV and a bond length of 0.25–0.46 nm. It is of great importance for non-polar surface interactions and hydrophobic forces.

4.2 Impacts on the overall properties of graphene-based nanocomposites

All four bridging mechanisms mentioned above are frequently involved in the synthesis of graphene-based nanocomposites or papers. In comparison to graphite or nanocomposites made from reduced graphene sheets, graphene oxide based composites feature much richer interlayer binding chemistry, such as hydrogen bonds between epoxy and hydroxyl groups on graphene basal planes, or covalent bonds through polymers (*e.g.* glutaraldehyde and alkylamines) in addition to the coordinative bonds we focus on here.

In order to improve the overall properties (modulus, strength and toughness) of graphene-based nanocomposites, three requirements should be fulfilled. (1) As the graphene sheets usually have a finite size of micrometers, an effective way to increase intralayer integration is needed for in-plane tension load transfer. (2) Due to the randomness in the distribution of the graphene sheet sizes, positions and stacking orders, the load transfer between adjacent graphene layers should be enhanced by introducing interlayer bridging. (3) The crosslink between graphene sheets should be able to re-associate after breaking under tensile or shear loads. This ensures a high toughness by utilizing the concept of 'sacrificial bonds' in biological materials such as bones. Additionally, one interesting observation in ref. 10 is that repeated cyclic loading of a metal-modified paper sample with small force and under slow rate may allow for chemically annealing to the best crosslink structure. Thus the reformation and adjustment of crosslinks under loads are of critical importance for the enhancement of the mechanical properties of these nanocomposites. To fulfil requirements (1) and (2), strong bonding, like covalent and coordinative bonds, take the advantage. However for (3), covalent bonds, which are very short-ranged and directional, are hard to reform after breaking. While the hydrogen bonds and van der Waals forces are much weaker. Thus coordinative bonds could play a critical role in this scenario with the presence of epoxy and hydroxyl groups on graphene oxide sheets.

One additional benefit from interlayer crosslinkers is that as they are introduced, the interlayer distance is expanded. In comparison to metallic materials such as aluminium with a mass density 2.7 g cm^{-3}, the density of graphite, 2.25 g cm^{-3}, is already lower. For structure I as an example, the expansion due to coordinative bonding will further lower the density by approximately half. The density could further be reduced by introducing larger-sized crosslinks, *e.g.* calcium based ones.

5. Conclusion

Based on the experimental observations as reported in ref. 10, we study the role of magnesium-mediated coordinative bonds in the mechanical properties enhancement of graphene-based nanocomposites, as summarized in Table 1. The balance between high strength and ability to reform after breaking gives these coordinative bonds unique potential in reinforcement applications. Our density functional theory based first-principles calculations give the detailed atomic structures and basic mechanical parameters of these coordinative bonds and illustrate the failure mechanism due to bond breaking at high loads. The quantified mechanical properties (modulus, strength and maximum strain in prior to structure failure) can be substituted into the micromechanical models to give the relationship between more complicated structures and the overall properties of whole composites. Also, the basic understanding of the coordinative bond mechanics here could be useful in studying similar structures in biological materials, for which more complicated environmental issues such as solvent effects (pH value, ionic effects *etc.*) need to be further explored.

6.Acknowledgements

This work is supported by Tsinghua University through the Key Talent Support Program, and the National Science Foundation of China through Young Scholar Grant 11002079.

References

1 D. Cai and M. Song, *J. Mater. Chem.*, 2010, **20**, 7906–7915.
2 R. Verdejo, M. M. Bernal, L. J. Romasanta and M. A. Lopez-Manchado, *J. Mater. Chem.*, 2011, **21**, 3301–3310.
3 J. W. C. Dunlop and P. Fratzl, *Annu. Rev. Mater. Res.*, 2010, **40**, 1–24.
4 P. M. Ajayan and J. M. Tour, *Nature*, 2007, **447**, 1066–1068.

View Online

5 S. Stankovich, D. A. Dikin, G. H. B. Dommett, K. M. Kohlhaas, E. J. Zimney, E. A. Stach, R. D. Piner, S. T. Nguyen and R. S. Ruoff, *Nature*, 2006, **442**, 282–286.
6 M. F. Yu, O. Lourie, M. J. Dyer, K. Moloni, T. F. Kelly and R. S. Ruoff, *Science*, 2000, **287**, 637–640.
7 D. Qian, W. K. Liu and R. S. Ruoff, *Compos. Sci. Technol.*, 2003, **63**, 1561–1569.
8 D. A. Dikin, S. Stankovich, E. J. Zimney, R. D. Piner, G. H. B. Dommett, G. Evmenenko, S. T. Nguyen and R. S. Ruoff, *Nature*, 2007, **448**, 457–460.
9 H. Jeong, Y. P. Lee, R. J. W. E. Lahaye, M. H. Park, K. H. An, I. J. Kim, C. Yang, C. Y. Park, R. S. Ruoff and L.Y.H., *J. Am. Chem. Soc.*, 2008, **130**, 5.
10 S. Park, K.-S. Lee, G. Bozoklu, W. Cai, S. T. Nguyen and R. S. Ruoff, *ACS Nano*, 2008, **2**, 572–578.
11 S. Stankovich, D. A. Dikin, R. D. Piner, K. A. Kohlhaas, A. Kleinhammes, Y. Jia, Y. Wu, S. T. Nguyen and R. S. Ruoff, *Carbon*, 2007, **45**, 1558–1565.
12 S. Stankovich, D. A. Dikin, O. C. Compton, G. H. B. Dommett, R. S. Ruoff and S. T. Nguyen, *Chem. Mater.*, 2010, **22**, 4153–4157.
13 J. M. Köhler and W. Fritzsche, *Nanotechnology: an introduction to nanostructuring techniques*, 1st edn, John Wiley & Sons, 2004.
14 J. Dong, J. M. Canfield, A. K. Mehta, J. E. Shokes, B. Tian, W. S. Childers, J. A. Simmons, Z. Mao, R. A. Scott, K. Warncke and D. G. Lynn, *Proc. Natl. Acad. Sci. U. S. A.*, 2007, **104**, 13313–13318.
15 K. Nakamoto, *Infrared and Raman Spectra of Inorganic and Coordination Compounds*, John Wiley & Sons, New York, 1986.
16 R. H. Telling, C. P. Ewels, A. A. El-Barbary and M. I. Heggie, *Nat. Mater.*, 2003, **2**, 333–337.
17 H. E. Troiani, M. Miki-Yoshida, G. A. Camacho-Bragado, M. A. L. Marques, A. Rubio, J. A. Ascencio and M. Jose-Yacaman, *Nano Lett.*, 2003, **3**, 751–755.
18 M. Conti, G. Falini and B. Samorì, *Angew. Chem., Int. Ed.*, 2000, **39**, 215–218.
19 S. Keten, Z. Xu, B. Ihle and M. J. Buehler, *Nat. Mater.*, 2010, **9**, 359–367.
20 Z. Xu and M. J. Buehler, *Nanotechnology*, 2009, **20**, 375704–8.
21 S. J. Grabowski, *Hydrogen Bonding - New Insights*, Springer, Dordrecht, 2006.

Published on 30 March 2011 on http://pubs.rsc.org | doi:10.1039/C1JM10300H
Downloaded by Tsinghua University on 28 April 2011

 This journal is © The Royal Society of Chemistry 2011